High concentrations of atmospheric isocyanic acid (HNCO) produced from secondary sources in China

Zelong Wang[1,2], Bin Yuan[1,2,*], Chenshuo Ye[3], James Roberts[4], Armin Wisthaler[5], Yi Lin[1,2], Tiange Li[1,2], Caihong Wu[1,2], Yuwen Peng[1,2], Chaomin Wang[1,2], Sihang Wang[1,2], Suxia Yang[1,2], Baolin Wang[6], Jipeng Qi[1,2], Chen Wang[6], Wei Song[7], Weiwei Hu[7], Xinming Wang[7], Wanyun Xu[8], Nan Ma[1,2], Ye Kuang[1,2], Jiangchuan Tao[1,2], Zhanyi Zhang[1,2], Hang Su[9], Yafang Cheng[9], Xuemei Wang[1,2], Min Shao[1,2,*]

[1] Institute for Environmental and Climate Research, Jinan University, Guangzhou 511443, China

[2] Guangdong-Hongkong-Macau Joint Laboratory of Collaborative Innovation for Environmental Quality

[3] State Joint Key Laboratory of Environmental Simulation and Pollution Control, College of Environmental Sciences and Engineering, Peking University, Beijing 100871, China

[4] NOAA Chemical Sciences Laboratory, Boulder, Colorado, 80305, USA

[5] Department of Chemistry, University of Oslo, P.O. Box 1033 Blindern, 0315 Oslo, Norway

[6] School of Environmental Science and Engineering, Qilu University of Technology (Shandong Academy of Sciences), Jinan 250353, China

[7] State Key Laboratory of Organic Geochemistry and Guangdong Key Laboratory of Environmental Protection and Resources Utilization, Guangzhou Institute of Geochemistry, Chinese Academy of Sciences, Guangzhou 510640, China

[8] State Key Laboratory of Severe Weather & Key Laboratory for Atmospheric Chemistry of China Meteorology Administration, Chinese Academy of Meteorological Sciences, Beijing 100081, China

[9] Multiphase Chemistry Department, Max Planck Institute for Chemistry, Mainz 55128, Germany

*Correspondence to: Bin Yuan (byuan@jnu.edu.cn) and Min Shao

(mshao@pku.edu.cn)

Abstract

Isocyanic acid (HNCO) is a potentially toxic atmospheric pollutant, whose atmospheric concentrations are hypothesized to be linked to adverse health effects. An earlier model study estimated that concentrations of isocyanic acid in China are highest around the world. However, measurements of isocyanic acid in ambient air have not been available in China. Two field campaigns were conducted to measure isocyanic acid in ambient air using a high-resolution time-of-flight chemical ionization mass spectrometer (ToF-CIMS) in two different environments in China. The ranges of mixing ratios of isocyanic acid are from below detection limit (18 pptv) to 2.8 ppbv (5 min average) with the average value of 0.46 ppbv at an urban site of Guangzhou in the Pearl River Delta (PRD) region in fall and from 0.02 ppbv to 2.2 ppbv with the average value of 0.37 ppbv at a rural site in the North China Plain (NCP) during wintertime, respectively. These concentrations are significantly higher than previous measurements in North America. The diurnal variations of isocyanic acid are very similar to secondary pollutants (e.g. ozone, formic acid and nitric acid) in PRD, indicating that isocyanic acid is mainly produced by secondary formation. Both primary emissions and secondary formation account for isocyanic acid in NCP. The lifetime of isocyanic acid in lower atmosphere was estimated to be less than one day due to the high apparent loss rate caused by deposition at night in PRD. Based on steady state analysis of isocyanic acid during the daytime, we show that amides are unlikely enough to explain the formation of isocyanic acid in Guangzhou, calling for additional precursors for isocyanic acid. Our measurements of isocyanic acid in two environments of China provide important constraints on the concentrations, sources and sinks of this pollutant in the atmosphere.

1. Introduction

Human health can be adversely affected by atmospheric pollutants, among which toxic components are one of the main culprits. Isocyanic acid (HNCO), as a trace gas in ambient air, can participate in the protein carbamylation reactions, leading to the development of cardiovascular impairment, cataracts and rheumatoid arthritis, via breath[1-5]. As isocyanic acid is highly soluble at physiological pH, it is estimated that ~1 ppbv is the upper limit of the inhaled isocyanic acid concentration, more than which it is sufficient to cause the protein carbamylation reactions at the interfaces of the atmosphere with the human body (e.g. the lungs)[6-8]. Thus, it is vital to accurately quantify concentrations of isocyanic acid in ambient air for a better understanding of variations, sources and sinks of isocyanic acid.

Since the first online measurements of isocyanic acid by chemical-ionization mass spectrometry from emissions of biomass burning and in ambient air[9], the knowledge on isocyanic acid has improved significantly[7]. The sources of isocyanic acid include primary emissions from biomass burning[6], diesel vehicles[10-12], gasoline vehicles[12, 13], extraction of oil sands[14] and cigarette smoke[15] and secondary formation in photochemical processes[16-22]. The known precursors for isocyanic acid include amides[22], amines[23], urea[24] and nicotine[21]. In general, amines are oxidized to amides and then amides are subsequently oxidized to isocyanates[19, 23]. Besides, diesel exhausts are also reported to form isocyanic acid substantially, although the components of diesel exhausts contributing to the increase of isocyanic acid are unknown[20]. The main sinks of isocyanic acid are dry and wet deposition[25-29]. Due to the high water solubility, isocyanic acid can be absorbed into the aqueous phase and then undergo hydrolysis to produce NH_3 and CO_2[18, 25, 27]. However, the understanding of the atmospheric fate of isocyanic acid is still incomplete, partially limited by the lack of measurement data in various environments.

The earliest global modelling study, which treated all isocyanic acid from biomass burning and anthropogenic emissions, predicted that parts of China would have the highest annual mean concentration (0.47 ppbv) of isocyanic acid around the world in

2008[30], while the latest global simulation demonstrates conflicting results with relatively lower concentrations (below 0.2 ppbv) of isocyanic acid over most parts of China[28]. These different modelling results, due mainly to the different emission inventories used to estimate the combustion sources of isocyanic acid, amplifies the need for measurements of isocyanic acid in ambient air in this region. In this study, in-situ measurements of isocyanic acid in ambient air were conducted in two different environments (urban and rural) in China. The concentration levels and diurnal variations of isocyanic acid were compared with previous measurement results in other regions. The implications on the sources and sinks of isocyanic acid in the atmosphere will be discussed.

2. Experimental

Isocyanic acid in ambient air was measured during two different field campaigns. One was conducted in September 25 – November 20 of 2018 at an urban site in Guangzhou (23.13°N, 113.26°E), a mega-city in Pearl River Delta (PRD) region. Another set of measurements was carried out at a rural site (38.85°N, 115.48°E) in North China Plain (NCP) in winter in November 26 – December 24, 2018. The detailed descriptions of the two sites are provided in Section S1 of the Supporting Information (SI). Supporting measurements were simultaneously performed including meteorological parameters, carbon monoxide (CO), nitrogen oxides (NO_x), ozone and VOCs measured by a proton transfer reaction time-of-flight mass spectrometer (PTR-ToF-MS) and an online gas chromatograph mass spectrometer/flame ionization detector (GC-MS/FID). The detailed setup of the PTR-ToF-MS and the GC-MS/FID is presented in Wu et al.[31]. The PTR-ToF-MS with H_3O^+ chemistry was calibrated by the standard gas with 16 VOC components every day during two campaigns. Formamide and C_2 amides were calibrated using a Liquid Calibration Unit (LCU) in the laboratory before the campaigns. The sensitivities of C_3 – C_{10} amides and methyl isocyanate were determined from the averaged sensitivity of the calibrated VOC compounds during the two campaigns. The detailed derivation process of the sensitivities and the specific

information of the calibrated compounds are provided by Wu et al.[31].

Isocyanic acid was measured by a high-resolution time-of-flight chemical ionization mass spectrometer with iodide reagent ion (I^- ToF-CIMS) utilizing X-rays as the ionization source. A 3-meter-long Teflon tubing (1/4") was used for sampling ambient air with a total flow of 9.0 L/min, 2.0 L/min of which was introduced into the ion-molecule reaction (IMR) region through an orifice. The IMR body was heated to 100 °C to reduce the wall loss on the inner surface. The pressures of the IMR and small segmented quadrupole (SSQ) were regulated at ~380 mbar and ~2.2 mbar, respectively. Isocyanic acid was detected as the iodide adduct, $IHNCO^-$, and quantified using the counts at m/z 169.9108 Th (Figure S2 in SI). Calibration was performed after the campaigns in the laboratory using a custom-built diffusion source by formation of HNCO from thermal decomposition of cyanuric acid ($C_3H_3N_3O_3$) at 300 °C[9, 32]. The delivered concentration of the diffusion source for isocyanic acid was determined using an ion chromatography method (see details in Section S2 of SI). The sensitivity of isocyanic acid was obtained to be 236 ± 3 ncps/ppbv at the dry condition, which is close to the value of about 250 ncps/ppbv derived from another I^- CIMS instrument[32]. The humidity dependence of the sensitivity of isocyanic acid in I^- ToF-CIMS was also obtained (Figure S6 in SI). During the two campaigns, the I^- ToF-CIMS was deployed with the filter inlet for gases and aerosols (FIGAERO). As a result, isocyanic acid and other gas phase species were measured for the first 24 minutes of each hour, with 21 minutes for ambient air and 3 minutes for background. The detection limits of isocyanic acid with an integration time of 5 min at a signal-to-noise ratio of 3 were 18 pptv and 8 pptv during the field campaigns in PRD and NCP, respectively. The total uncertainty of isocyanic acid measurements was estimated to be < 25% (see details in section S2 of SI). In addition to isocyanic acid, formic acid and nitric acid were simultaneously measured by the I^- ToF-CIMS during the two campaigns. Formic acid was calibrated using the LCU before the campaigns and nitric acid was calibrated in the laboratory after the campaigns with a permeation tube. The calibration of levoglucosan was conducted by injecting liquid standards with different concentration onto the filter of FIGAERO manually.

3. Results and Discussion

3.1 Concentration levels of isocyanic acid

The average mixing ratios of isocyanic acid in the gas phase in PRD and NCP were 0.46 ± 0.41 ppbv and 0.37 ± 0.19 ppbv, respectively. The mixing ratio measured at the two sites are compared with previous measurements in the literature, as shown in Figure 1 (also in Table S1 and Figure S7 of SI). As urban sites, the average mixing ratio of isocyanic acid in PRD were one order of magnitude higher than Los Angeles, USA (0.025 ppbv)[6, 17] and Calgary, Canada (0.036 ppbv)[32]. The mixing ratio of isocyanic acid in PRD ranged from below detection limit (18 pptv) to 2.8 ppbv (5 min average). The maximum mixing ratio in PRD was measured on October 11, 2018, the day with highest daily average mixing ratio of isocyanic acid (1.8 ± 0.5 ppbv) during the entire campaign. At the rural site, the mixing ratio of isocyanic acid ranged from 0.02 ppbv to 2.2 ppbv (5 min average). The maximum mixing ratio was detected in the plume on December 22, 2018. The average mixing ratio of isocyanic acid in NCP is also six times higher than the values (0.055 ppbv) measured at rural sites in USA (e.g. Fort Collins)[17]. Besides, the number of days exceeding the mixing ratio threshold of 1 ppbv was used to assess the pollution level of isocyanic acid[30]. There were 20 days with the maximum mixing ratio (5 min average) of isocyanic acid exceeding 1 ppbv in PRD, accounting for more than one third (38%) of the total observation days. The exceedance days in NCP were less than in PRD, with 5 days exceeding 1 ppbv in the total of 29 days of measurements.

In summary, the concentration of isocyanic acid in China is much higher than that in Canada and USA, which is significantly different from the latest global simulation results that the concentrations of isocyanic acid in North American are higher than those in China[28]. The only two measurements showing higher than our results shown in this study are from suburban sites influenced by crop residue burning in India[33] and in Nepal[34]. However, the instruments (i.e. PTR-ToF-MS) used for measurements in India and Nepal were not explicitly calibrated for isocyanic acid and the water dependence

in the PTR-ToF-MS response to isocyanic acid was also not taken into account (discussed in Section S2 of SI)[22, 35, 36]. Note that the early global chemistry transport model predicted an annual mean concentration of isocyanic acid in the range of 0.2 to 0.5 ppbv in PRD and NCP[30]. Although the modelled concentrations are comparable to our *in situ* measurements, the model treated all of isocyanic acid source as primary emissions by simple scaling to HCN that is usually co-emitted with HNCO. As discussed in the following parts, our observations show a significant fraction of isocyanic acid comes from secondary production.

As the I^- ToF-CIMS was equipped with a FIGAERO, isocyanic acid in particle phase was also measured (Figure S7 in SI). The average concentrations of isocyanic acid in the particle phase were 0.001 ± 0.001 ppbv during the PRD campaign and 0.005 ± 0.006 ppbv during the NCP campaign, respectively. Accordingly, the average fractions in the particle phase (F_p) were 0.004 ± 0.005 in PRD and 0.015 ± 0.021 in NCP. The higher F_p in NCP than in PRD is probably due to the higher concentrations of organic aerosol in NCP (37.2 ± 26.3 μg/m^3) than in PRD (14.8 ± 8.7 μg/m^3) and the lower temperature in NCP (0.5 ± 3.6 °C) than in PRD (24.3 ± 3.2 °C)[37]. Since the lifetime of isocyanic acid against hydrolysis in aqueous phase ranges from five hours to over a month at atmospherically relevant water pH values and temperatures[7], the low F_p in both sites suggests that only a very small portion of gaseous isocyanic acid were absorbed into the particle phase, which is consistent with the judgement that the partition into wet aerosol is not a significant sink for gaseous isocyanic acid due to the low aerosol liquid water content[25]. As the concentrations of isocyanic acid in the particle phase were rather low, this study mainly focused on the isocyanic acid in the gas phase.

3.2 Diurnal variations of isocyanic acid

Diurnal variations of isocyanic acid along with other air pollutants, including CO, NO_x, O_3 and O_x (i.e. O_3+NO_2), measured at the two sites are shown in Figure 2. The concentration of isocyanic acid in PRD showed a pronounced diurnal profile with highest concentrations in the afternoon. The diurnal profile of isocyanic acid was very

200 similar to many secondary pollutants, including O_3 and O_x, but clearly different from
201 primary species, e.g. CO, NO_x and hydrocarbons (Figure S9 in SI), which exhibited
202 higher concentrations at night and lower ones in the daytime. The comparisons of
203 diurnal variations of isocyanic acid and levoglucosan, a tracer of biomass burning,
204 indicates that the high daytime concentration of isocyanic acid was unlikely from
205 biomass burning (Figure S10 in SI). As the fraction in particle phase (F_p) for isocyanic
206 acid was below 0.04 throughout the PRD campaign (Figure S7 and Figure S8 in SI),
207 the gas-particle partitioning contributed little to the increase of gaseous isocyanic acid
208 during the daytime. Thus, we conclude that isocyanic acid was predominately produced
209 by secondary formation during the campaign in PRD.
210 Diurnal variations of isocyanic acid in NCP were obviously different from those in
211 PRD. Concentrations of isocyanic acid were relative stable throughout the day, with
212 somewhat higher concentrations in the morning. This diurnal profile of isocyanic acid
213 was different from both primary pollutants (CO, NO_x, hydrocarbon and acetonitrile)
214 and secondary pollutants (O_3, O_x and HNO_3) shown in Figure 2 and Figure S9 - S11 of
215 SI. The primary pollutants had much higher concentrations at night and lowest
216 concentrations in the afternoon, while secondary pollutants show higher concentrations
217 in the afternoon. In addition, isocyanic acid had moderate correlations with both CO
218 ($r=0.57$) and O_x ($r=0.65$) during the NCP campaign (Figure S14 and Figure S16 in SI).
219 These observations suggest isocyanic acid in NCP had contributions from both primary
220 emissions and secondary formation.
221 Diurnal profile analysis indicates sources of isocyanic acid are different between
222 measurements in PRD and NCP. This is also reflected by correlations of isocyanic acid
223 with CO, O_3 and O_x during two campaigns (Figure S14 - S16 in SI). Moderate
224 correlation between isocyanic acid and CO is observed in NCP, while little correlation
225 is obtained in PRD. In addition to the differences between urban and rural sites, the
226 different seasons of the two campaigns also have an important impact on the sources of
227 isocyanic acid. Furthermore, we also conduct a combined analysis of diurnal profiles
228 for isocyanic acid in different environments, based on reported data in the literature
229 (Figure S13 in SI). We observed large variability in diurnal variations observed in

different environments, indicating the complexity of sources influencing the concentrations of isocyanic acid in ambient air.

3.3 High loss rates of isocyanic acid at night

As shown in Figure 2, we observed a strong diurnal profile of isocyanic acid in PRD during the campaign, with much higher concentrations during the daytime. After reaching the concentration plateau in the afternoon (14:00 - 16:00), the concentrations of isocyanic acid started to decrease in the evening until midnight. The time series of isocyanic acid in October 12-19 also clearly demonstrated this phenomenon, as shown in Figure 3. Along with isocyanic acid, we also observe similar quick decline of concentrations for nitric acid, formic acid and ozone, which results in good correlations with each other at night (Figure S17 in SI). As the measurements were conducted at the urban site with strong primary emissions, the decline of ozone in the evening is the result of titration by local NO emission. However, there are no known gas-phase chemical loss pathways for the three acids that can induce the decline of concentration at night. Considering that these acids are highly water-soluble and it is not the rainy season during the campaign, this evidence suggests that there must be some losses (e.g. dry deposition) contributing to the concentration decline in the evening.

Here, we extract the daily data between 19:00 and 24:00, and use an exponential curve to derive the apparent loss rate for isocyanic acid, along with nitric acid and formic acid, which is detailedly described in Section S9 of SI. Four typical cases measured during the PRD campaign were shown in Figure S20. The average value of the apparent loss rates for isocyanic acid at every night with an obvious decline in concentrations was calculated to be 0.39 ± 0.12 h^{-1}, equivalent to a lifetime of 2.6 ± 0.8 h for isocyanic acid in the nocturnal boundary layer. The apparent loss rates for formic acid and nitric acid are calculated as 0.28 ± 0.04 h^{-1} and 0.44 ± 0.08 h^{-1} using the same method, respectively.

The average boundary layer height in the evening is estimated to be ~400 m during the campaign based on the NOAA HYSPLIT model (Figure S21 in SI), which is consistent with observations of average nocturnal boundary layer height in Guangzhou

259 measured by Micro Pulse Lidar[38]. Using the equation of the deposition velocity (V_d)[39] :

260 $$V_d = \frac{h}{\tau} \quad (1)$$

261 where h is the boundary layer height and τ is the lifetime of isocyanic acid, it can be
262 roughly estimated that the deposition velocity for isocyanic acid is 4.3 ± 1.3 cm/s in the
263 evening. Based on the same method, the deposition velocities for formic acid and nitric
264 acid are estimated to be 3.1 ± 0.4 cm/s and 4.9 ± 0.9 cm/s. The determined deposition
265 velocities for these water-soluble acids are consistent with previous parameterization
266 of dry deposition (4.2 cm/s for formic acid and 5.1 cm/s for nitric acid)[39, 40].

267 The deposition velocity during the daytime is usually higher than that at night[39], as
268 the result of the strong convection during the daytime. If we assume a similar daytime
269 deposition velocity as nighttime and using the same eq 1 with the average boundary
270 layer height of 1000 m during the day (Figure S21 in SI), the lifetime of isocyanic acid
271 due to deposition is estimated to be 6.5 ± 2.0 h in the day (corresponding to loss rate of
272 0.15 ± 0.05 h^{-1}).

273 Here, we perform a back-of-the-envelope estimate for the longest effective lifetime
274 of isocyanic acid throughout the day. A simplified atmospheric structure of boundary
275 layer is supposed, consisting of daytime boundary layer, nocturnal boundary layer and
276 nocturnal residual layer (Figure S22). The average boundary layer height of 1000 m
277 during the daytime is used. During the nighttime, the average boundary layer height
278 decreases to 400 m and the nocturnal residual layer with a height of 600 m appears
279 (Figure S21). It is assumed that C_{HNCO} is the concentration of isocyanic acid at the end
280 of the daytime in the entire boundary layer. The concentration of isocyanic acid in the
281 nocturnal boundary layer would decrease with the loss rate of 0.39 ± 0.12 h^{-1} by dry
282 deposition (the orange curve in Figure S22). As the night lasts for 12 hours, using the
283 equation of $C = C_{HNCO} * e^{-kt}$ (k=0.39 h^{-1}, t=12 h), the concentration in the nocturnal
284 boundary layer would be $0.01 * C_{HNCO}$ in the morning. The concentration of isocyanic
285 acid in the nocturnal residual layer would be still C_{HNCO} in the morning (the green
286 curve in Figure S22) with the negligible loss as discussed in Section S11 of SI.
287 Assuming a prompt atmospheric mixing between the nocturnal boundary layer and

residual layer, the concentration of isocyanic acid in the convective boundary layer would be $0.60 * C_{HNCO}$ in the morning after the convective boundary layer develops. Thus, it would take additional 3.2 h for the concentration of isocyanic acid to decrease to $1/e * C_{HNCO}$ with the loss rate of 0.15 ± 0.05 h^{-1} in the daytime (the red curve in Figure S22). Therefore, the effective lifetime for isocyanic acid in ambient air would be less than 16 h, which is slightly shorter than about one day of lifetime estimated for deposition to neutral pH surfaces in boundary layer[27]. As shown in the discussions in Section S11 of SI, the assumptions underlying the calculation affect little on the conclusion that the effective lifetime for isocyanic acid would be less than 16 h. To sum up, the effective lifetime for isocyanic acid mainly against dry deposition ranges from 6 h to 16 h in ambient air.

3.4 Strong secondary formation of isocyanic acid and possible precursors

Based on discussions in section 3.2 and 3.3, we observed both strong secondary formation and deposition during the PRD campaign. As the concentrations of isocyanic acid show a plateau without obvious variations in the afternoon (14:00-16:00), we can apply a steady state analysis to evaluate the rates of secondary formation for isocyanic acid during this period[17]:

$$[HNCO]k_{loss} = Emisson_{HNCO} + \sum k_{precursor}[OH][Precursor]Y_{HNCO} \quad (2)$$

where $[HNCO]k_{loss}$, $Emisson_{HNCO}$ and $\sum k_{precursor}[OH][Precursor]Y_{HNCO}$ represent loss rates, primary emission rates and secondary formation rates for isocyanic acid, respectively. According to the discussion in Section S8 of SI, the contribution of primary emission to isocyanic acid was below 10% in the afternoon. Then, assuming that $Emisson_{HNCO}$ was 10% of the total production rate of isocyanic acid, the steady-state equation can be derived to:

$$[HNCO]k_{loss} * 0.9 = \sum k_{precursor}[OH][Precursor]Y_{HNCO} \quad (3)$$

where $[HNCO]$, $[Precursor]$, $[OH]$ are the average concentration of isocyanic acid, its precursors and OH radicals in 14:00-16:00, respectively. The average concentration of OH radical between 14:00 and 16:00 (3.0 ± 1.3 × 10^6 molecule cm^{-3}) is determined

317 from simulation using a box model with MCM v3.3.1 as chemical mechanism and
318 constraints of observed VOCs, NO_x and other environmental parameters during the
319 PRD campaign[31, 37] (Section S12 of SI). k_{loss} is the first order loss rate of isocyanic
320 acid. Here, we use the inverse of lifetime due to deposition determined in section 3.3
321 for the daytime (0.15 ± 0.05 h^{-1}). $k_{precursor}$ is the rate coefficients for the reactions of
322 OH radicals with the precursors of isocyanic acid. Y_{HNCO} is the yields of isocyanic acid
323 from oxidation of precursors.

324 Using the average isocyanic acid concentration of 0.67 ± 0.02 ppbv in 14:00-16:00,
325 we can estimate production rates of isocyanic acid should be 0.090 ± 0.030 ppb/h to
326 maintain its concentration during this period (Figure 4a). Amides has been identified as
327 important precursors of isocyanic acid[17, 22-24]. Using measured concentrations of
328 formamide, C_2 amides, C_3 amides C_4 amides and $C_5 - C_{10}$ amides by PTR-ToF-MS
329 along with the reported yield of isocyanic acid from these amides, the production rate
330 of isocyanic acid was rather low ($(4.4 \pm 1.7) \times 10^{-3}$ ppb/h, Figure 4a and Table S3 in SI),
331 which is significantly lower than the production rate needed to maintain isocyanic acid
332 concentration. We also considered another extreme case that assumes all nitrogen in
333 amides is converted to isocyanic acid as the upper limit of production for isocyanic
334 acid. Using this method, the production rate is determined as 0.038 ± 0.013 ppb/h,
335 which is significantly enhanced compared to production rate from amides determined
336 using reported yield. However, this production rate is still significantly lower than the
337 rate needed to maintain its concentration in this period. This result suggests that there
338 must be some other precursors contributing to secondary formation of isocyanic acid.
339 Several previous studies also reported that secondary formation of isocyanic acid is
340 higher than expected[17, 18, 41], though contributions from different precursors are
341 considered in these studies. In addition to amides, other nitrogen-containing organic
342 compounds may account for the "missing" formation of isocyanic acid. For example,
343 oxidation of urea[24], monoethanolamine[16] and nicotine[21] in the atmosphere is reported
344 to form isocyanic acid without going through an amide intermediate. However, these
345 nitrogen-containing species (urea, moethanolamine and nicotine) were not observed

346 with significant signals by PTR-ToF-MS during the campaign.

347 It is interesting to observe that concentrations of C_3 amides are largest among
348 amides and C_3 amides account for 74% of the production rate for isocyanic acid from
349 all amides if assuming all nitrogen in amides is converted to isocyanic acid (Figure 4a).
350 The C_3 amides measured by PTR-ToF-MS (m/z 74.0600, $C_3H_7NOH^+$) showed
351 relatively high concentrations during the campaign with a maximum of 5.6 ppbv (1 h
352 average) observed on October 25, 2018. The diurnal variations of C_3 amides exhibited
353 higher concentrations at night and lower concentrations during the daytime. This
354 diurnal profile is similar to various primary species during the campaign, as shown in
355 Figure 2. A recent study also observed large signals of m/z 74 in mass spectra of PTR-
356 MS at a site in an industrial region of Guangzhou, about 16 kilometers east of our
357 measurement site[42]. Owing to low mass resolution of the PTR-MS used in that study,
358 the signals at m/z 74 were tentatively attributed to butylamine ($C_4H_{11}N$) with the
359 average concentration of 123 ppbv[42]. Based on the high-resolution peak fitting of m/z
360 74 for mass spectra of PTR-ToF-MS (Figure S25 in SI), we confirmed that the signals
361 at m/z 74 are mainly from C_3 amides, rather than butylamine. Among various VOCs
362 species, we observe good correlations between C_3 amides and styrene, another tracer of
363 emissions from industrial sources[43, 44]. It implies that C_3 amides were mainly from
364 industrial emissions[45]. Among various isomers of C_3 amides, N,N-dimethylformamide
365 is known to be used as solvents and intermediates involved in a variety of industrial
366 applications, including the manufacture of pharmaceuticals, pesticides, fibers and
367 films[24, 46]. The diurnal variations of methyl isocyanate, a first or second generation of
368 photo-oxidation products of C_2 to C_4 amides[19, 24, 47], were very close to that of isocyanic
369 acid (Figure S12 in SI).

370 In summary, concentrations and diurnal variations of isocyanic acid in ambient air
371 were obtained in two field campaigns in China, which makes the scarce measurements
372 of isocyanic acid more extensive, especially in East Asia, an area for which there are
373 conflicting model estimates. The average concentration of isocyanic acid in Guangzhou
374 is about one order of magnitude higher than those in North America. We show that
375 isocyanic acid in Guangzhou is largely induced by the secondary formation, validating

the recent proposal that photochemical sources of isocyanic acid could be more significant than primary sources in urban areas[20]. The secondary formation process of isocyanic acid must be considered in the model study, otherwise the simulation results will be severely underestimated in some areas. Based on steady state analysis, formation of isocyanic acid from amides is shown to be significantly lower than the production rate to maintain concentration of isocyanic acid, indicating additional precursors for isocyanic acid are needed. The diurnal analysis of isocyanic acid also indicates rapid dry deposition of isocyanic acid, which strongly limits the lifetime of isocyanic acid in the lower atmosphere. Our measurements of isocyanic acid in two environments of China provide important constraints on the concentrations, sources and sinks of this pollutant in the atmosphere.

Supporting Information

Detailed information on measurement sites, calibrations for isocyanic acid, comparisons of isocyanic acid with other pollutants, calculations of apparent loss rates, discussions of the effective lifetime for isocyanic acid, simulations of OH radicals and production rates from different precursors of isocyanic acid.

Acknowledgements

This work was supported by the National Natural Science Foundation of China (grant No. 41877302), the National Key R&D Plan of China (grant No. 2018YFC0213904, 2016YFC0202206), Guangdong Natural Science Funds for Distinguished Young Scholar (grant No. 2018B030306037), Key-Area Research and Development Program of Guangdong Province (grant No. 2019B110206001), Guangdong Soft Science Research Program (2019B101001005), Guangdong Innovative and Entrepreneurial Research Team Program (grant No. 2016ZT06N263) and Guangdong Basic and Applied Basic Research Fund Project (grant No. 2019A1515110792). Weiwei Hu was supported by National Natural Science Foundation of China (41875156). J. Roberts was supported by NOAA's Climate Research and Health of the Atmosphere Initiative.

403 # Reference

404 1. Mydel, P.; Wang, Z.; Brisslert, M.; Hellvard, A.; Dahlberg, L. E.; Hazen, S. L.;
405 Bokarewa, M., Carbamylation-Dependent Activation of T Cells: A Novel Mechanism
406 in the Pathogenesis of Autoimmune Arthritis. *The Journal of Immunology* **2010,** *184*,
407 (12), 6882.
408 2. Beswick, H. T.; Harding, J. J., Conformational changes induced in bovine lens
409 alpha-crystallin by carbamylation. Relevance to cataract. *The Biochemical journal*
410 **1984,** *223*, (1), 221-227.
411 3. Verbrugge, F. H.; Tang, W. H. W.; Hazen, S. L., Protein carbamylation and
412 cardiovascular disease. *Kidney International* **2015,** *88*, (3), 474-478.
413 4. Wang, Z.; Nicholls, S. J.; Rodriguez, E. R.; Kummu, O.; Hörkkö, S.; Barnard, J.;
414 Reynolds, W. F.; Topol, E. J.; DiDonato, J. A.; Hazen, S. L., Protein carbamylation
415 links inflammation, smoking, uremia and atherogenesis. *Nature Medicine* **2007,** *13*,
416 1176.
417 5. Koeth, R. A.; Kalantar-Zadeh, K.; Wang, Z.; Fu, X.; Tang, W. H. W.; Hazen, S.
418 L., Protein Carbamylation Predicts Mortality in ESRD. *Journal of the American Society*
419 *of Nephrology* **2013,** *24*, (5), 853-861.
420 6. Roberts, J. M.; Veres, P. R.; Cochran, A. K.; Warneke, C.; Burling, I. R.; Yokelson,
421 R. J.; Lerner, B.; Gilman, J. B.; Kuster, W. C.; Fall, R.; de Gouw, J., Isocyanic acid in
422 the atmosphere and its possible link to smoke-related health effects. *Proceedings of the*
423 *National Academy of Sciences* **2011,** *108*, (22), 8966-8971.
424 7. Leslie, M. D.; Ridoli, M.; Murphy, J. G.; Borduas-Dedekind, N., Isocyanic acid
425 (HNCO) and its fate in the atmosphere: a review. *Environmental Science: Processes &*
426 *Impacts* **2019,** *21*, (5), 793-808.
427 8. Plehiers, P. M., Comment on "Isocyanic acid (HNCO) and its fate in the
428 atmosphere: a review" by M. D. Leslie, M. Ridoli, J. G. Murphy and N. Borduas-
429 Dedekind, Environ. Sci.: Processes Impacts, 2019, 21, 793. *Environmental Science:*
430 *Processes & Impacts* **2019,** *21*, (12), 2150-2152.
431 9. Roberts, J.; Veres, P.; Warneke, C.; Neuman, J. A.; Washenfelder, R. A.; Brown,

S. S.; Baasandorj, M.; Burkholder, J. B.; Burling, I. R.; Johnson, T. J.; Yokelson, R. J.; de Gouw, J., Measurement of HONO, HNCO, and other inorganic acids by negative-ion proton-transfer chemical-ionization mass spectrometry (NI-PT-CIMS): application to biomass burning emissions. *Atmos. Meas. Tech.* **2010,** *3*, (4), 981-990.

10. Wentzell, J. J. B.; Liggio, J.; Li, S.-M.; Vlasenko, A.; Staebler, R.; Lu, G.; Poitras, M.-J.; Chan, T.; Brook, J. R., Measurements of Gas phase Acids in Diesel Exhaust: A Relevant Source of HNCO? *Environmental Science & Technology* **2013,** *47*, (14), 7663-7671.

11. Jathar, S. H.; Heppding, C.; Link, M. F.; Farmer, D. K.; Akherati, A.; Kleeman, M. J.; de Gouw, J. A.; Veres, P. R.; Roberts, J. M., Investigating diesel engines as an atmospheric source of isocyanic acid in urban areas. *Atmos. Chem. Phys.* **2017,** *17*, (14), 8959-8970.

12. Wren, S. N.; Liggio, J.; Han, Y.; Hayden, K.; Lu, G.; Mihele, C. M.; Mittermeier, R. L.; Stroud, C.; Wentzell, J. J. B.; Brook, J. R., Elucidating real-world vehicle emission factors from mobile measurements over a large metropolitan region: a focus on isocyanic acid, hydrogen cyanide, and black carbon. *Atmos. Chem. Phys.* **2018,** *18*, (23), 16979-17001.

13. Brady, J. M.; Crisp, T. A.; Collier, S.; Kuwayama, T.; Forestieri, S. D.; Perraud, V.; Zhang, Q.; Kleeman, M. J.; Cappa, C. D.; Bertram, T. H., Real-Time Emission Factor Measurements of Isocyanic Acid from Light Duty Gasoline Vehicles. *Environmental Science & Technology* **2014,** *48*, (19), 11405-11412.

14. Liggio, J.; Stroud, C. A.; Wentzell, J. J. B.; Zhang, J.; Sommers, J.; Darlington, A.; Liu, P. S. K.; Moussa, S. G.; Leithead, A.; Hayden, K.; Mittermeier, R. L.; Staebler, R.; Wolde, M.; Li, S.-M., Quantifying the Primary Emissions and Photochemical Formation of Isocyanic Acid Downwind of Oil Sands Operations. *Environmental Science & Technology* **2017,** *51*, (24), 14462-14471.

15. Hems, R. F.; Wang, C.; Collins, D. B.; Zhou, S.; Borduas-Dedekind, N.; Siegel, J. A.; Abbatt, J. P. D., Sources of isocyanic acid (HNCO) indoors: a focus on cigarette smoke. *Environmental Science: Processes & Impacts* **2019,** *21*, (8), 1334-1341.

16. Borduas, N.; Abbatt, J. P. D.; Murphy, J. G., Gas Phase Oxidation of

462 Monoethanolamine (MEA) with OH Radical and Ozone: Kinetics, Products, and
463 Particles. *Environ. Sci. Technol.* **2013,** *47*, (12), 6377-6383.
464 17. Roberts, J. M.; Veres, P. R.; VandenBoer, T. C.; Warneke, C.; Graus, M.; Williams,
465 E. J.; Lefer, B.; Brock, C. A.; Bahreini, R.; Öztürk, F.; Middlebrook, A. M.; Wagner,
466 N. L.; Dubé, W. P.; Gouw, J. A., New insights into atmospheric sources and sinks of
467 isocyanic acid, HNCO, from recent urban and regional observations. *Journal of*
468 *Geophysical Research: Atmospheres* **2014,** *119*, (2), 1060-1072.
469 18. Zhao, R.; Lee, A. K. Y.; Wentzell, J. J. B.; Mcdonald, A. M.; Toom-Sauntry, D.;
470 Leaitch, W. R.; Modini, R. L.; Corrigan, A. L.; Russell, L. M.; Noone, K. J.; Schroder,
471 J. C.; Bertram, A. K.; Hawkins, L. N.; Abbatt, J. P. D.; Liggio, J., Cloud partitioning of
472 isocyanic acid (HNCO) and evidence of secondary source of HNCO in ambient air.
473 *Geophysical Research Letters* **2014,** *41*, (19), 6962-6969.
474 19. Borduas, N.; da Silva, G.; Murphy, J. G.; Abbatt, J. P. D., Experimental and
475 Theoretical Understanding of the Gas Phase Oxidation of Atmospheric Amides with
476 OH Radicals: Kinetics, Products, and Mechanisms. *J. Phys. Chem. A* **2015,** *119*, (19),
477 4298-4308.
478 20. Link, M. F.; Friedman, B.; Fulgham, R.; Brophy, P.; Galang, A.; Jathar, S. H.;
479 Veres, P.; Roberts, J. M.; Farmer, D. K., Photochemical processing of diesel fuel
480 emissions as a large secondary source of isocyanic acid (HNCO). *Geophysical*
481 *Research Letters* **2016,** *43*, (8), 4033-4041.
482 21. Borduas, N.; Murphy, J. G.; Wang, C.; da Silva, G.; Abbatt, J. P. D., Gas Phase
483 Oxidation of Nicotine by OH Radicals: Kinetics, Mechanisms, and Formation of
484 HNCO. *Environmental Science & Technology Letters* **2016,** *3*, (9), 327-331.
485 22. Bunkan, A. J. C.; Mikoviny, T.; Nielsen, C. J.; Wisthaler, A.; Zhu, L., Experimental
486 and Theoretical Study of the OH-Initiated Photo-oxidation of Formamide. *The Journal*
487 *of Physical Chemistry A* **2016,** *120*, (8), 1222-1230.
488 23. Lee, D.; Wexler, A. S., Atmospheric amines – Part III: Photochemistry and toxicity.
489 *Atmos. Environ.* **2013,** *71*, 95-103.
490 24. Barnes, I.; Solignac, G.; Mellouki, A.; Becker, K. H., Aspects of the Atmospheric
491 Chemistry of Amides. *ChemPhysChem* **2010,** *11*, (18), 3844-3857.

492 25. Borduas, N.; Place, B.; Wentworth, G. R.; Abbatt, J. P. D.; Murphy, J. G.,
493 Solubility and reactivity of HNCO in water: insights into HNCO's fate in the
494 atmosphere. *Atmos. Chem. Phys.* **2016,** *16*, (2), 703-714.
495 26. Barth, M. C.; Cochran, A. K.; Fiddler, M. N.; Roberts, J. M.; Bililign, S., Numerical
496 modeling of cloud chemistry effects on isocyanic acid (HNCO). *Journal of Geophysical*
497 *Research: Atmospheres* **2013,** *118*, (15), 8688-8701.
498 27. Roberts, J. M.; Liu, Y., Solubility and solution-phase chemistry of isocyanic acid,
499 methyl isocyanate, and cyanogen halides. *Atmos. Chem. Phys.* **2019,** *19*, (7), 4419-4437.
500 28. Rosanka, S.; Vu, G. H. T.; Nguyen, H. M. T.; Pham, T. V.; Javed, U.; Taraborrelli,
501 D.; Vereecken, L., Atmospheric chemical loss processes of isocyanic acid (HNCO): a
502 combined theoretical kinetic and global modelling study. *Atmos. Chem. Phys.* **2020,** *20*,
503 (11), 6671-6686.
504 29. Fulgham, S. R.; Millet, D. B.; Alwe, H. D.; Goldstein, A. H.; Schobesberger, S.;
505 Farmer, D. K., Surface Wetness as an Unexpected Control on Forest Exchange of
506 Volatile Organic Acids. **2020,** *47*, (15), e2020GL088745.
507 30. Young, P. J.; Emmons, L. K.; Roberts, J. M.; Lamarque, J.-F.; Wiedinmyer, C.;
508 Veres, P.; VandenBoer, T. C., Isocyanic acid in a global chemistry transport model:
509 Tropospheric distribution, budget, and identification of regions with potential health
510 impacts. *Journal of Geophysical Research-Atmospheres* **2012,** *117*.
511 31. Wu, C.; Wang, C.; Wang, S.; Wang, W.; Yuan, B.; Qi, J.; Wang, B.; Wang, H.;
512 Wang, C.; Song, W.; Wang, X.; Hu, W.; Lou, S.; Ye, C.; Peng, Y.; Wang, Z.; Huangfu,
513 Y.; Xie, Y.; Zhu, M.; Zheng, J.; Wang, X.; Jiang, B.; Zhang, Z.; Shao, M., Measurement
514 Report: important contributions of oxygenated compounds to emissions and chemistry
515 of VOCs in urban air. *Atmos. Chem. Phys. Discuss.* **2020,** *2020*, 1-37.
516 32. Woodward-Massey, R.; Taha, Y. M.; Moussa, S. G.; Osthoff, H. D., Comparison
517 of negative-ion proton-transfer with iodide ion chemical ionization mass spectrometry
518 for quantification of isocyanic acid in ambient air. *Atmos. Environ.* **2014,** *98*, 693-703.
519 33. Chandra, B. P.; Sinha, V., Contribution of post-harvest agricultural paddy residue
520 fires in the N.W. Indo-Gangetic Plain to ambient carcinogenic benzenoids, toxic
521 isocyanic acid and carbon monoxide. *Environment International* **2016,** *88*, 187-197.

522 34. Sarkar, C.; Sinha, V.; Kumar, V.; Rupakheti, M.; Panday, A.; Mahata, K. S.;
523 Rupakheti, D.; Kathayat, B.; Lawrence, M. G., Overview of VOC emissions and
524 chemistry from PTR-TOF-MS measurements during the SusKat-ABC campaign: high
525 acetaldehyde, isoprene and isocyanic acid in wintertime air of the Kathmandu Valley.
526 *Atmos. Chem. Phys.* **2016,** *16*, (6), 3979-4003.
527 35. Yuan, B.; Koss, A. R.; Warneke, C.; Coggon, M.; Sekimoto, K.; de Gouw, J. A.,
528 Proton-Transfer-Reaction Mass Spectrometry: Applications in Atmospheric Sciences.
529 *Chem. Rev.* **2017,** *117*, (21), 13187-13229.
530 36. Jankowski, M. J.; Olsen, R.; Nielsen, C. J.; Thomassen, Y.; Molander, P., The
531 applicability of proton transfer reaction-mass spectrometry (PTR-MS) for
532 determination of isocyanic acid (ICA) in work room atmospheres. *Environmental*
533 *Science: Processes & Impacts* **2014,** *16*, (10), 2423-2431.
534 37. Wang, C.; Wu, C.; Wang, S.; Qi, J.; Wang, B.; Wang, Z.; Hu, W.; Chen, W.; Ye,
535 C.; Wang, W.; Sun, Y.; Wang, C.; Huang, S.; Song, W.; Wang, X.; Yang, S.; Zhang,
536 S.; Xu, W.; Ma, N.; Zhang, Z.; Jiang, B.; Su, H.; Cheng, Y.; Wang, X.; Shao, M.; Yuan,
537 B., Measurements of higher alkanes using NO+PTR-ToF-MS: significant contributions
538 of higher alkanes to secondary organic aerosols in China. *Atmos. Chem. Phys. Discuss.*
539 **2020,** *2020*, 1-32.
540 38. Song, L.; Deng, T.; Wu, D.; He, G.; Sun, J.; Weng, J.; Wu, C., Study on planetary
541 bounary layer height in a typical haze period and different weather types over
542 Guangzhou. *Acta Scientiae Circumstantiae* **2019,** *39*, (5), 1381-1391.
543 39. Nguyen, T. B.; Crounse, J. D.; Teng, A. P.; St. Clair, J. M.; Paulot, F.; Wolfe, G.
544 M.; Wennberg, P. O., Rapid deposition of oxidized biogenic compounds to a temperate
545 forest. *Proceedings of the National Academy of Sciences* **2015,** *112*, (5), E392-E401.
546 40. Zhang, L.; Brook, J. R.; Vet, R., A revised parameterization for gaseous dry
547 deposition in air-quality models. *Atmos. Chem. Phys.* **2003,** *3*, (6), 2067-2082.
548 41. Kumar, V.; Chandra, B. P.; Sinha, V., Large unexplained suite of chemically
549 reactive compounds present in ambient air due to biomass fires. *Scientific Reports* **2018,**
550 *8*, (1), 626.
551 42. Luo, H.; Li, G.; Chen, J.; Lin, Q.; Ma, S.; Wang, Y.; An, T., Spatial and temporal

552 distribution characteristics and ozone formation potentials of volatile organic
553 compounds from three typical functional areas in China. *Environ. Res.* **2020,** *183*,
554 109141.
555 43. Guo, H.; Wang, T.; Louie, P. K. K., Source apportionment of ambient non-methane
556 hydrocarbons in Hong Kong: Application of a principal component analysis/absolute
557 principal component scores (PCA/APCS) receptor model. *Environ. Pollut.* **2004,** *129*,
558 (3), 489-498.
559 44. Miller, R. R.; Newhook, R.; Poole, A., Styrene Production, Use, and Human
560 Exposure. *Crit. Rev. Toxicol.* **1994,** *24*, (sup1), S1-S10.
561 45. Yao, L.; Wang, M. Y.; Wang, X. K.; Liu, Y. J.; Chen, H. F.; Zheng, J.; Nie, W.;
562 Ding, A. J.; Geng, F. H.; Wang, D. F.; Chen, J. M.; Worsnop, D. R.; Wang, L.,
563 Detection of atmospheric gaseous amines and amides by a high-resolution time-of-
564 flight chemical ionization mass spectrometer with protonated ethanol reagent ions.
565 *Atmos. Chem. Phys.* **2016,** *16*, (22), 14527-14543.
566 46. Kennedy, G. L., Toxicology of dimethyl and monomethyl derivatives of acetamide
567 and formamide: a second update. *Crit. Rev. Toxicol.* **2012,** *42*, (10), 793-826.
568 47. Bunkan, A. J. C.; Hetzler, J.; Mikoviny, T.; Wisthaler, A.; Nielsen, C. J.; Olzmann,
569 M., The reactions of N-methylformamide and N,N-dimethylformamide with OH and
570 their photo-oxidation under atmospheric conditions: experimental and theoretical
571 studies. *PCCP* **2015,** *17*, (10), 7046-7059.
572 48. Mungall, E. L.; Abbatt, J. P. D.; Wentzell, J. J. B.; Lee, A. K. Y.; Thomas, J. L.;
573 Blais, M.; Gosselin, M.; Miller, L. A.; Papakyriakou, T.; Willis, M. D.; Liggio, J.,
574 Microlayer source of oxygenated volatile organic compounds in the summertime
575 marine Arctic boundary layer. *Proceedings of the National Academy of Sciences* **2017,**
576 *114*, (24), 6203-6208.
577

578 Table of Contents (TOC) Art

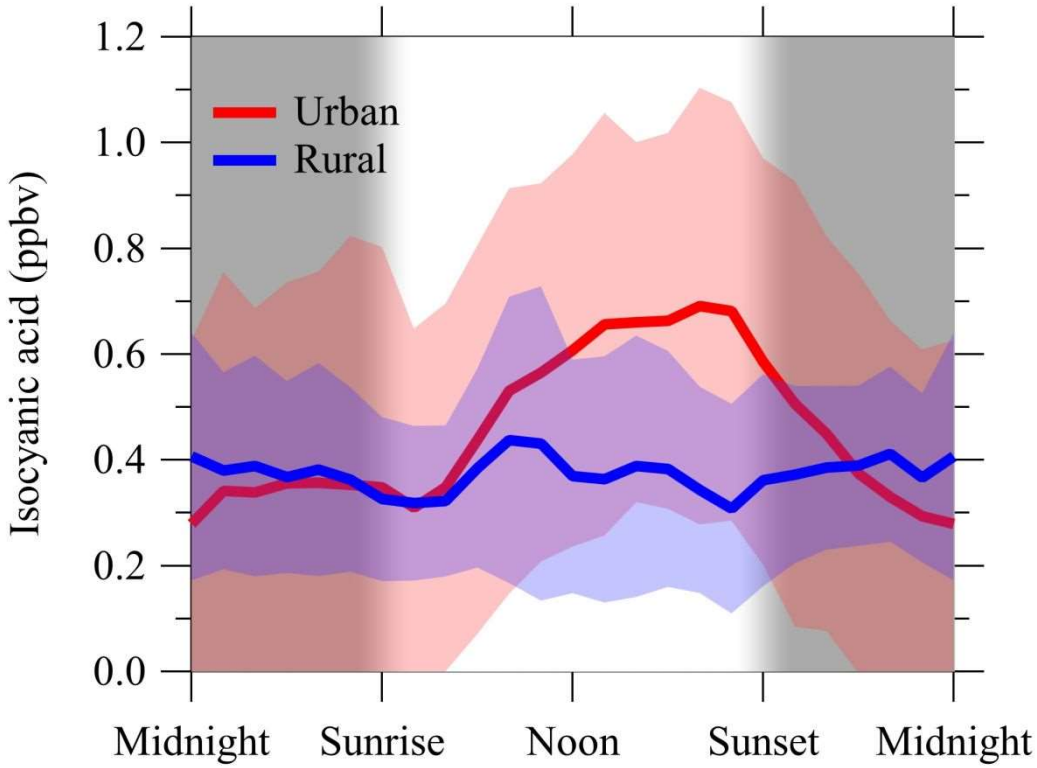

579

580

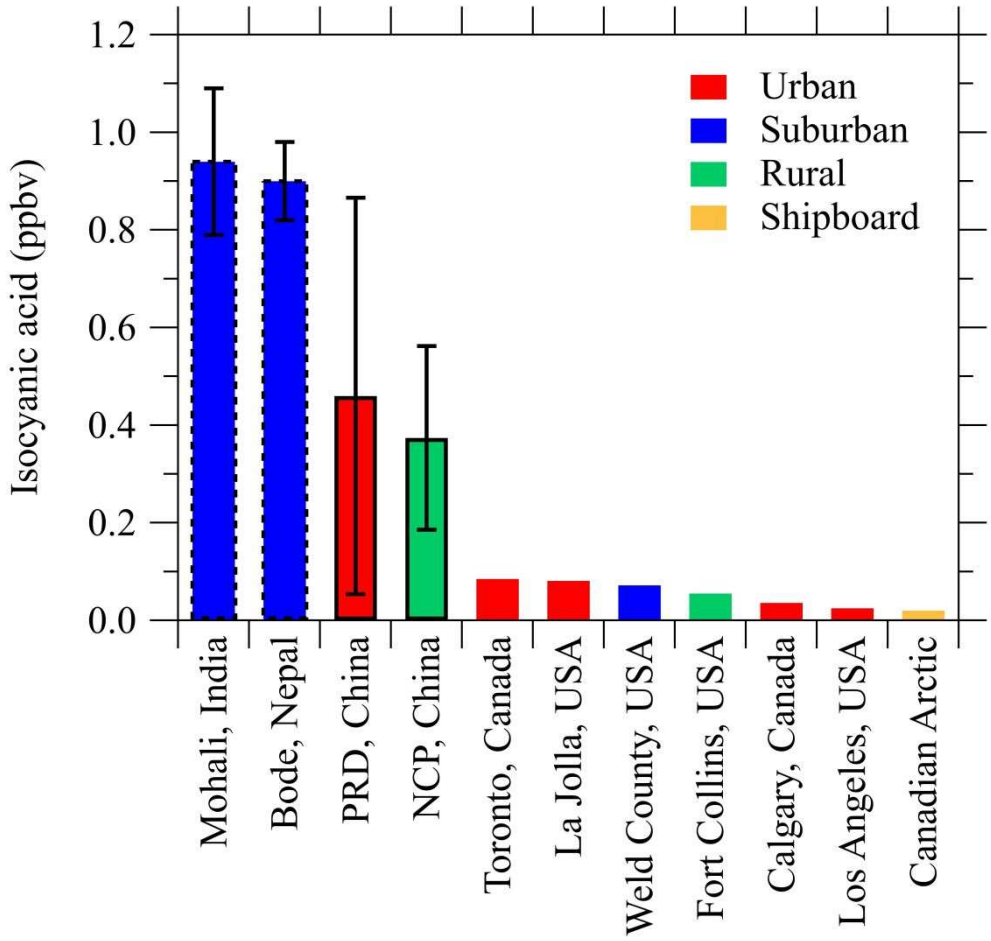

581

582 **Figure 1.** Comparisons of mean concentration levels of isocyanic acid in this study
583 (PRD and NCP) and results reported in previous studies (Mohali[33], Bode[34], Toronto[10],
584 La Jolla[18], Weld County[17], Fort Collins[17], Calgary[32], Los Angeles[17] and Arctic[48]). The
585 data of isocyanic acid measured at Mohali, India[33] and Bode, Nepal[34] are shown with
586 the dashed box, as these data were not explicitly calibrated for isocyanic acid.

587

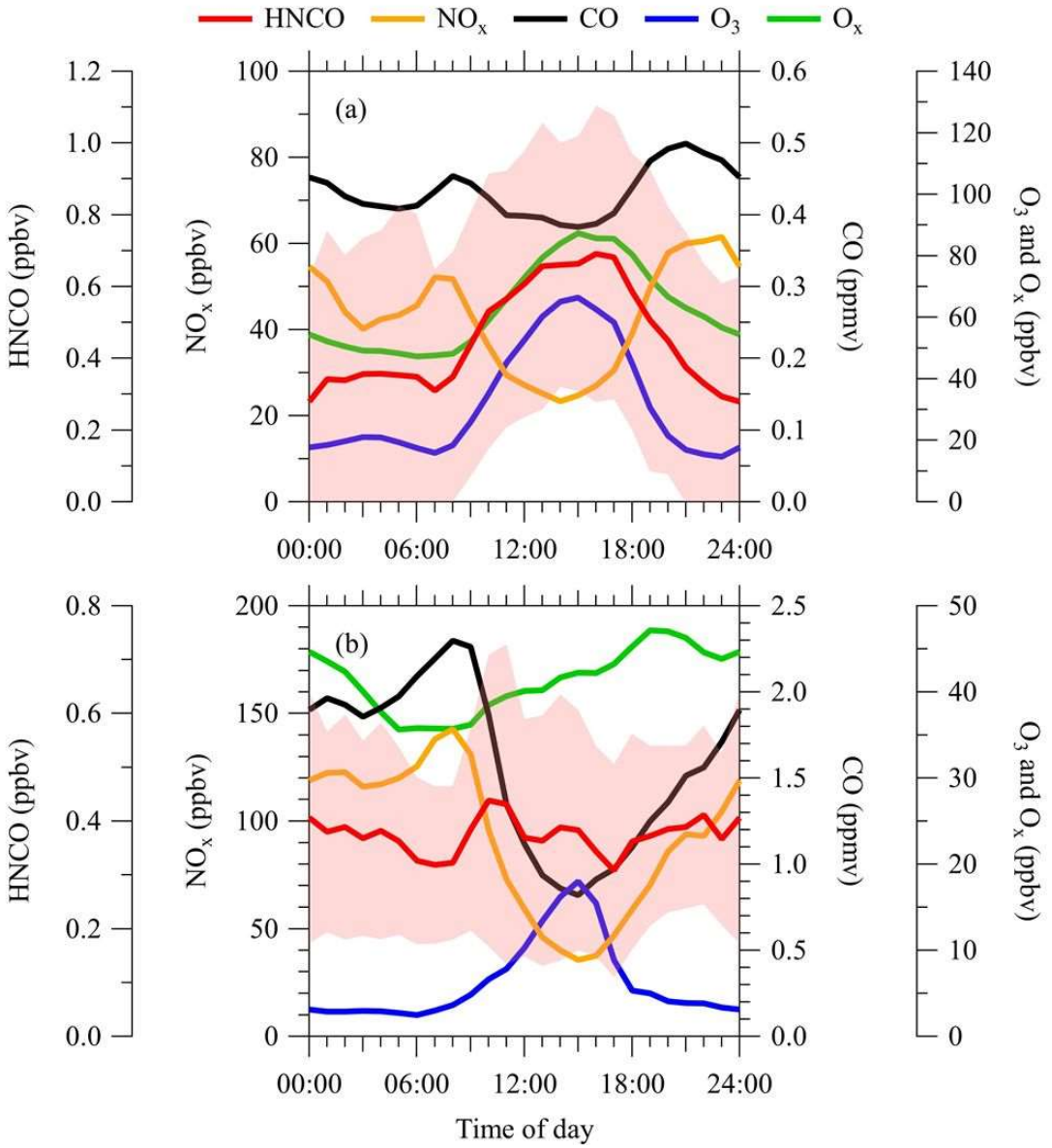

588

589 **Figure 2.** Average diurnal variations of isocyanic acid, CO, NO_x, O_3 and O_x in (a)

590 PRD and (b) NCP. The shaded areas represent standard deviations of 1 h average for

591 isocyanic acid.

592

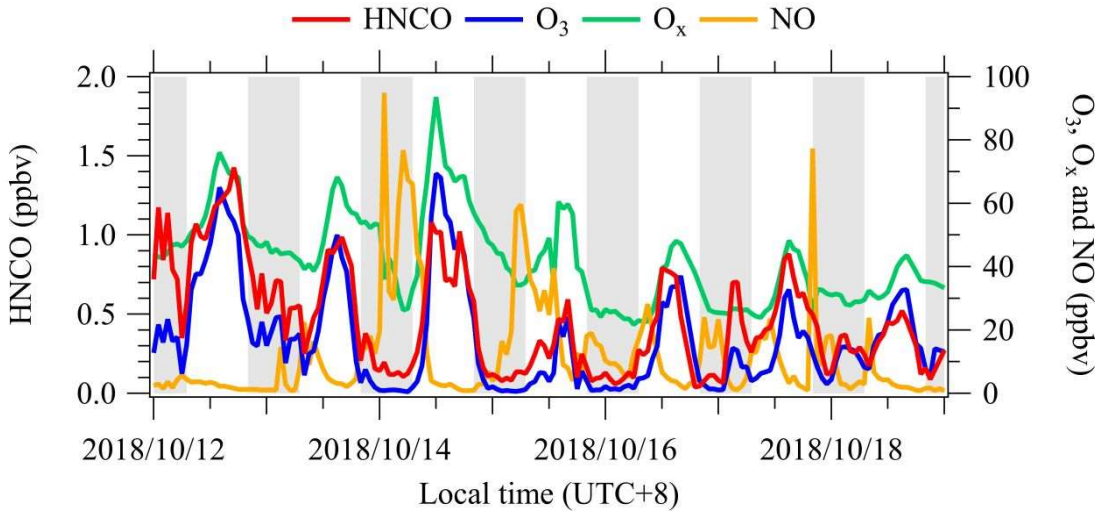

Figure 3. Time series of isocyanic acid, ozone, O_x and NO for part of the study period in PRD. The grey regions represent the nighttime (before 07:00 and after 19:00).

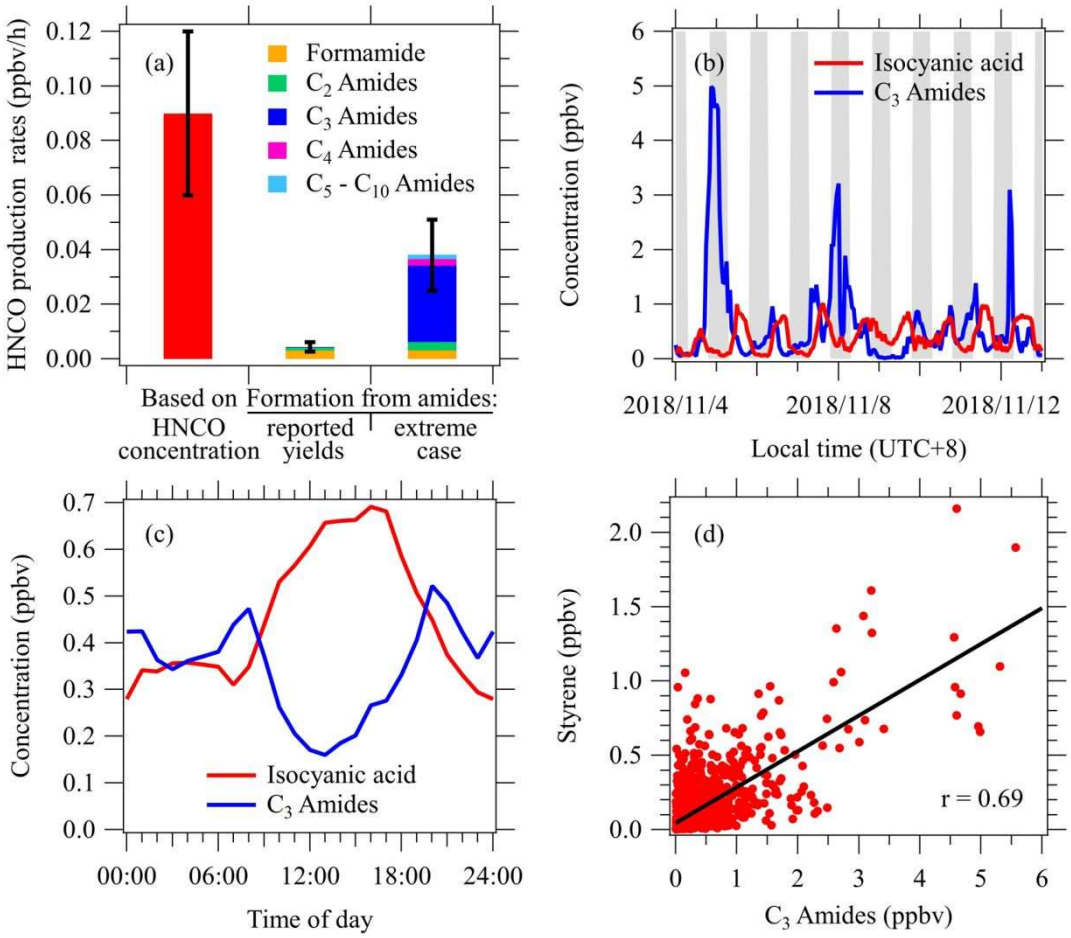

Figure 4. Amides as precursors of isocyanic acid during the PRD campaign. (a) Comparison of the determined isocyanic acid production rates from steady state analysis and calculated contributions from various amides during 14:00-16:00. Reported yields: production rate determined from reported yields of amides. Extreme case: production rate determined assuming all nitrogen in amide is converted to isocyanic acid (i.e. yield is 100%). (b) Time series of isocyanic acid and C_3 amides for part of the study period in PRD. The grey regions represent the nighttime (before 07:00 and after 19:00). (c) Comparisons of diurnal variation profiles between C_3 amides and isocyanic acid. (d) Correlations of C_3 amides with styrene during the entire PRD campaign.